

Boron and nitrogen doping in graphene for the catalysis of acetylene hydrochlorination

Bin Dai, Kun Chen, yang wang, Lihua Kang, and Mingyuan Zhu

ACS Catal., Just Accepted Manuscript • DOI: 10.1021/acscatal.5b00199 • Publication Date (Web): 15 Mar 2015

Downloaded from <http://pubs.acs.org> on March 17, 2015

Just Accepted

“Just Accepted” manuscripts have been peer-reviewed and accepted for publication. They are posted online prior to technical editing, formatting for publication and author proofing. The American Chemical Society provides “Just Accepted” as a free service to the research community to expedite the dissemination of scientific material as soon as possible after acceptance. “Just Accepted” manuscripts appear in full in PDF format accompanied by an HTML abstract. “Just Accepted” manuscripts have been fully peer reviewed, but should not be considered the official version of record. They are accessible to all readers and citable by the Digital Object Identifier (DOI®). “Just Accepted” is an optional service offered to authors. Therefore, the “Just Accepted” Web site may not include all articles that will be published in the journal. After a manuscript is technically edited and formatted, it will be removed from the “Just Accepted” Web site and published as an ASAP article. Note that technical editing may introduce minor changes to the manuscript text and/or graphics which could affect content, and all legal disclaimers and ethical guidelines that apply to the journal pertain. ACS cannot be held responsible for errors or consequences arising from the use of information contained in these “Just Accepted” manuscripts.



**Boron and nitrogen doping in graphene for the catalysis of acetylene
hydrochlorination**

Bin Dai^{a, b}, Kun Chen^a, Yang Wang^a, Lihua Kang^{a, b}, Mingyuan Zhu^{a, b} *

^aSchool of Chemistry and Chemical Engineering of Shihezi University, Shihezi,
Xinjiang, 832000, RP China.

^bKey Laboratory for Green Processing of Chemical Engineering of Xinjiang Bingtuan,
Shihezi, Xinjiang, 832000, RP China.

*Corresponding author. Tel.: +86 9932057270; Fax: +86 9932057210.

E-mail address: zhumin yuan@shzu.edu.cn (M. Zhu)

Abstract: Exploration of environmental-friendly catalysts is important for acetylene hydrochlorination, due that the traditional HgCl_2 catalyst is highly toxic and harmful to human health. Herein, boron and nitrogen heteroatoms dual doped on oxide graphene (B, N-G) catalyst was synthesized using a model calcination method and applied as a non-metallic catalyst for acetylene hydrochlorination. The B, N-G catalyst shows acetylene conversion significantly higher (nearly 95%) than that of singly B- or N-doped graphenes and a little lower than that of Au and Hg catalyst. Density functional theory calculations and temperature-programmed desorption results indicate that the synthetic effect of B and N doping can promote HCl adsorption, which is the rate-determining step in acetylene hydrochlorination. The excellent catalytic efficiency and relatively low cost of B, N-G makes it a promising catalyst for acetylene hydrochlorination.

Keywords: Nitrogen and boron doping; Graphene; Metal-free catalyst; Acetylene hydrochlorination; HCl adsorption

1
2
3
4
5
6
7
8
9
10
11
12
13
14
15
16
17
18
19
20
21
22
23
24
25
26
27
28
29
30
31
32
33
34
35
36
37
38
39
40
41
42
43
44
45
46
47
48
49
50
51
52
53
54
55
56
57
58
59
60

1. Introduction

Polyvinylchloride (PVC) polymerization from vinyl chloride monomer (VCM) is one of the most widely used engineering plastics in various aspects of human life, and is suitable for numerous manufacturing various products, such as water pipes and fittings, electric wires, and plastic membranes. The domestic industrial production of VCM in China is mainly through calcium carbide method (acetylene hydrochlorination), and the reaction is catalyzed by carbon-supported mercuric chloride catalyst. However, the toxic mercuric chloride causes serious environmental problems and harm to human health [1]. Therefore, the extended studies on environmental-friendly catalysts have attracted increasing interest and are important for the industrial application of acetylene hydrochlorination.

Considerable catalytic activity has been achieved on some chloride of transition metals, such as Au [2], Bi [3], and Pt [4], towards acetylene hydrochlorination. Hutchings et al. [5, 6] found that Au/AC has the best activity among these transition metals. Hutchings et al. also achieved an optimized catalytic activity when the catalyst contains 1 wt.% Au, although the poor stability of an Au catalyst still could not meet the criteria for industrial application [7-9]. As Au catalyst is expensive and scarce, exploitation of low-cost catalysts may be another development strategy for acetylene hydrochlorination catalyst [10, 11].

Recently, several N-doped carbons materials have been applied as novel heterogeneous catalysts for acetylene hydrochlorination. In our previous work [12], we reported that the acetylene conversion on g-C₃N₄/AC catalyst is about 70% that of

Au/AC catalyst. Wei et al. [13] similarly found that N-doped carbon nanotubes (N-CNTs) enhances the formation of the covalent bond between C_2H_2 and N-CNTs, and therefore promotes the catalytic activity for acetylene hydrochlorination. Recently, Bao et al. [14] reported that a nanocomposite of N-doped carbon derived from silicon carbide ($SiC@N-C$) directly activates acetylene hydrochlorination, has stable activity during acetylene conversion, which can reach 80%, and has vinyl chloride selectivity over 98% at 200 °C. Although N-doped carbon has considerable catalytic activity, its acetylene conversion is still lower than that of Au/AC and Hg/AC catalysts.

In the last few years, N-doped graphene materials gained substantial attention as catalyst for oxygen reduction reactions (ORR) [15-19]. Studies have reported that by sequentially incorporating N and B into selected sites of the graphene domain enhances the synergistic coupling effect that facilitates the catalytic ORR. In this study, N, B dual doped graphene was prepared through a two-step method, and the obtained catalyst showed a catalytic activity for acetylene hydrochlorination that is only a little lower than that of Au catalyst.

2. Experimental

2.1 Chemicals and reagents

Graphite powder (99.85%, J&K Chemical), Boric Acid (H_3BO_3 , 99.5%, J&K Chemical), C_2H_2 (gas, 98%), HCl (gas, $\geq 99\%$) were used in the present study.

2.2 Catalyst preparation

Graphene oxide (GO) was prepared according to classical Hummers method [20-22]. Graphite powder (5 g) was pretreated by the solution of concentrated H_2SO_4

(30 mL), $K_2S_2O_8$ (2.5 g), and P_2O_5 (2.5 g). The pre-oxidized graphite powder was added into H_2SO_4 (120 mL) solution and stirred for 10 min under ice bath. Then, $KMnO_4$ (18 g) was added gradually under stirring and the temperature of the mixture was kept to be below $\sim 15^\circ C$ by ice cooling, the mixture was stirred at $35^\circ C$ for 2 h. After diluted with deionized water (250 mL), the mixture was stirred for 2 h successively. The reaction was cooled to room temperature and poured onto 400 mL of cold deionized water. Successively, 20 mL of fresh 30% H_2O_2 was added, until observation of the mixture color changed into brilliant yellow along with bubbling, which indicating the complete oxidation of graphite. The resultant solution was centrifuged to obtain the product. The product was washed by 10% HCl aqueous solution and deionized water. The GO powder was collected by lyophilization for further characterizations and experiments.

To prepare the B-doped graphene (B-G), GO powder was mixed with excess boric acid in an Al_2O_3 combustion boat and was heated to $900^\circ C$ under flowing Ar for 5 h with a heating rate of $5^\circ C/min$. After annealing, the furnace was cooled to room temperature under the flowing Ar, and then the residual B_2O_3 was removed by washing with the boiling water. N-doped graphene (N-G) was synthesized by annealing GO powder under 20% NH_3/Ar at $900^\circ C$ for 5 h. A two-step B, N co-doping of graphene was achieved by annealing the pre-synthesized B-G intermediate under 20% NH_3/Ar at $900^\circ C$ for 5 h.

2.3 Catalyst characterization

Physical characterization of the sample was performed using a transmission

electron microscope (TEM, JEOL, JEM 2010 operating at 200 kV) for its morphological features. X-ray photoelectron spectroscopy (XPS) measurements were performed using an Axis Ultra spectrometer with a monochromatized Al K α X-ray as the excitation source (225W). Temperature-programmed desorption (TPD) was conducted using a Micromeritic ASAP 2720 instrument over a temperature ramp of 50 °C to 600°C, ramp rate of 10 °C/min, and flow rate of 40 mL/min under nitrogen atmosphere. Thermo gravimetric analysis (TGA) was conducted with TGA/DTA system (SDT Q600, America) at room temperature to 900 °C with air flow of 10 mL/min. The Raman spectra were obtained using a Raman spectrometer (Renishaw) with 514.3 nm Ar laser.

2.4 Catalytic performance evaluation

The catalyst performance evaluation was performed in a fixed bed microreactor (i.d. of 10mm). Before initiating the reaction, the reactor was purged with nitrogen to remove water and air in the reaction system. Hydrogen chloride gas was passed through the pipeline at a flow rate of 20 mL/min to activate the catalyst (0.5 g) until the microreactor was heated to 150°C. Afterward, acetylene and hydrogen chloride were fed through the microreactor, producing a gas hourly space velocity (GHSV, C₂H₂) of 36 h⁻¹. The exit gas mixture was passed through an absorption bottle containing clean water, and injected into a Shimadzu GC-2014C chromatograph for analysis. The conversion of acetylene (X_A) and the selectivity to VCM (S_{VC}) as the criteria of catalytic performance were defined as following equations [9], respectively.

$$X_A = \frac{\phi_{A0} - \phi_A}{\phi_{A0}} \times 100\% \quad (1)$$

$$S_{VC} = \frac{\phi_{VC}}{1 - \phi_A} \times 100\% \quad (2)$$

In the equations, ϕ_{A0} is defined as the volume fraction of acetylene in the raw gas and ϕ_A is defined as the volume fraction of remaining acetylene in the product gas, ϕ_{VC} is the volume fraction of vinyl chloride in product gas.

The turn over frequency (TOF) of acetylene as the criteria of catalytic performance was calculated using the following equation.

$$TOF = \frac{n_{C_2H_2}}{n_N \times t} \quad (3)$$

2.5 Computational details

DFT calculations were performed using the hybrid B3LYP [23, 24] function, as implemented in the Gaussian 09 computer program package [25]. The standard 6-311G ++** basis set was used for H, C, N, B and Cl atoms. Atomic charges were calculated using the Mulliken type. The geometries of all structures involved in the mechanism were optimized fully without any restrictions. The frequencies of all geometries were calculated at the same level to identify the nature of the stationary points and obtain the zero-point-energy (ZPE) corrections. All stationary points were characterized as minima (no imaginary frequencies) via Hessian calculation. An important reference point for this calculation is the adsorption energy for HCl on N-G and B, N-G. In this paper, we used the following definitions for adsorption energy. When HCl is adsorbed on graphene (N-G and B, N-G), the adsorption energy is calculated as:

$$E = E_{(system)} - E_{(G)} - E_{(HCl)} \quad (4)$$

$E_{(system)}$ is the total energy of adsorption system; $E_{(G)}$ denotes the energy of N-G or B,

N-G; $E_{(\text{HCl})}$ is the energy of HCl, respectively.

3. Results and discussions

Fig. 1a-c shows the TEM images that display the typical structures and morphologies of GO, N-G, and B, N-G transparent sheets with wrinkled and voile-like features. Despite of the pristine GO with the substitution of several carbon atoms with heteroatoms, the nanosheet morphology was preserved. Fig. 2a shows the room temperature Raman spectra for pristine GO, N-G, and B, N-G at 514.3 nm excitation. The I_G/I_D is a known parameter of carbon materials, which is important in evaluating the degree of graphitization. The G band at 1597 cm^{-1} originates from the bond stretching of all sp^2 -bonded pairs, and the D band at 1352 cm^{-1} is associated with the sp^3 defect sites. The graphite-induced G-band notably shows a sequential decrease in intensity, which suggests that the increasing presence of N or B heteroatoms in the target is, in fact, bringing about a noticeable change in the ordering degree of the hexagonal lattice. These results are consistent with those of a previous report [26-28].

The XPS survey spectrum of the elemental compositions of GO, B-G, N-G, and B, N-G shown in Fig. 2b, which presents a predominant C1s peak (284.5 eV) and an O1s peak (532.0 eV). The detailed list showing the results of the quantitative evaluations performed through XPS confirms the existence of elemental N and B in the different graphene samples (Table1). Unlike undoped graphene, all the N-doped graphene samples show a visible N1s peak (399.5eV). The N levels in N-G, and B, N-G, are 5.47%, and 10.96%, respectively. These results suggest nitrogen can be incorporated in-situ into the sp^2 hybridized network in the presence of NH_3 . Similarly, the binding

energy values coincide with the data from literature [26, 29]. The XPS results together with that of Raman spectroscopy strongly confirmed that N and B atoms were successfully introduced into the graphene framework through covalent bonds.

To gain more insight into molecular structure of N/B-bonding configurations, detailed scans for the N1s and B1s, including their deconvolutions from high-resolution XPS, are shown in Fig. 2c-d. Compared with the N1s of N-G (Supporting information, Figure S1), high-resolution N1s peaks of B, N-G down-shifted to a lower binding energy. The lowest binding energy (398.0 eV) in the N1s spectrum is related to N-B bonded groups, which means that first with B and then to N can results boron nitride species. In addition, B, N-G have two split peaks in the high-resolution XPS B1s spectrum, the main peak at around 188.9 eV is attributable to BC₃, indicating that B heteroatoms have been successfully incorporated into the graphene lattice network. The B-N chemical bonds have also been observed in 190.9 eV [30, 31].

Under the same reaction conditions, the catalytic activity of GO, B-G, N-G, and B, N-G catalysts were evaluated using a fixed bed reactor, and the results are shown in Fig.3a. The figure shows that the initial acetylene conversion has the following trend: B, N-G > N-G > B-G > GO. Pristine GO showed negligible acetylene conversion (12.07%), and the acetylene conversion of B-G is only 26.96%, indicating that the B dopant has minimal effect on the catalytic activity on GO. However, N-G displays a substantially higher catalytic activity, and its acetylene conversion reach 62.74%. Numerous literatures have reported that N-doped carbon acts as a non-precious

catalyst for acetylene hydrochlorination [12-14]. Li et al. reported that the acetylene conversion of graphitic carbon nitride (g-C₃N₄/AC) was about 45% at a GHSV of 50 h⁻¹, and the catalytic performance of N-G for acetylene hydrochlorination is similar with those reported in literature. Dual-doped B, N-G catalyst interestingly exhibits an acetylene conversion of 94.98%, indicating that the B atom improves the catalytic activity of N-G for acetylene hydrochlorination. Supporting information, Figure S2, exhibited excellent selectivity of the singly/doubly doped graphenes for vinyl chloride monomers (at more than 98%) throughout the process, while pristine GO had a slightly lower selectivity. To compare the capacity of chlorinating C₂H₂ into VCM, the turn over frequency (TOF) value of metal-based catalysts (including Au, Hg), as well as the N-G and B, N-G metal-free catalysts are illustrated in Fig. 3b. The TOFs of N-G and B, N-G catalysts were $8.33 \times 10^{-3} \text{ min}^{-1}$ and $3.32 \times 10^{-2} \text{ min}^{-1}$, respectively. TOF of SiC@N-C catalyst reported by Bao et al. was about $5.63 \times 10^{-3} \text{ min}^{-1}$ [14], and that of C₃N₄ material in our previous work was $1.42 \times 10^{-2} \text{ min}^{-1}$ [12]. Those results indicate that the acetylene hydrochlorination rate on B, N-G is somewhat higher than the previous reported catalysts. From Fig. 3b, it can also be seen that the TOF of Au/AC and Hg/AC are 5.38 min^{-1} and 0.22 min^{-1} , respectively, being close to the literature [8]. It can be concluded the catalytic performance of B, N-G is about 15% of Hg/AC and 6‰ of Au/AC catalyst. The addition of the second heteroatoms has minimal effect on the selectivity, but dramatically enhances the catalytic activity. Both experimental and theoretical studies reveal that the carbon atoms bonded with N species are the active sites, and the schematic illustration of acetylene

hydrochlorination for B, N-G catalysts was shown in Fig. 4, more details of which would be stated subsequently.

The high catalytic activity of the doubly doped graphene layers in the acetylene hydrochlorination can be ascribed to the following two reasons: First, B, N-G provides more active sites compared with N-G because B, N-G has higher N content than N-G according to the results shown in Table 1; and second, the presence of B atom changes the electronic state of N atom (Supporting information, Figure S3) and thus affects the adsorption of HCl on N active sites because the adsorption of chloride molecule is the rate-determining step of the acetylene hydrochlorination process.

It is well known that GO is in abundance of oxygen atoms, in order to elucidate the effect of oxygen containing group on the catalytic performance, we build some valid models of GO, N-G, B, N-G with and without the presence of O atom, and the results was listed in Table S1 and Figure S4. These models are based on a previous study about oxygen reduction reaction on a hetero-doped graphene [18, 26]. From the aforementioned XPS analysis, three N species were considered and investigated because these N species significantly differ in terms of their structures. Different from traditional Hg and Au catalyst, carbon atom acts as the adsorbing site for C_2H_2 , and nitrogen atom provides the catalytic active site for HCl. Therefore, the carbon atoms bonded with N species are the active sites. As shown in Table S1, the presence of oxygen atom on N-G and B, N-G catalysts decrease the adsorption of HCl. As the adsorption of HCl is the rate determining step of acetylene hydrochlorination, it can be inferred that suggesting that no obvious promoting effect is present for oxygen

containing group on graphene layer. DFT calculations were also carried out to gain the fundamental understanding on the adsorption of acetylene (Supporting information, Figure S5). Theoretically results demonstrated that B-doping hardly enhanced the adsorption of acetylene, however, the various N species that interact with HCl have extremely different functions. Different species of N in the catalytic active sites for HCl adsorption (E_{ads}) were identified in Fig. 3c. For N-G, a two-fold coordinated pyridinic N dopant at the edge of the cluster had a specific and dominant HCl adsorption capability. However, no significant HCl adsorption capacity was observed with pyrrolic N, which agrees with the results of previous studies [12]. For dual-doped B, N-G, a higher E_{ads} value than those surveyed for N-G in both three types N was observed, suggesting that the catalyst enhanced the acetylene hydrochlorination reaction and thereby supports the above-discussed experimental results. The previously identified inactive pyrrolic N atom can boost HCl adsorption because of the coupling interaction between pyridinic N and B, which is shown by the dramatically increasing adsorption energy. The transition of pyrrolic N group from “inactive” into “active” after B incorporation can provide a better catalytic activity compared with N-G for the acetylene hydrochlorination. This result highlights the importance of B in the reaction. As for the graphitic N atom at the center of graphene layers, the energy of HCl are minimal, the hydrogen chloride molecule is hardly adsorbed at the active site of graphitic nitrogen. Furthermore, there are no obvious promoting effect between graphitic N and B atom.

Temperature-programmed desorption was performed to directly compare the

adsorption and activation of HCl on different graphenes. The desorption temperature in the TPD profiles reflects the binding strength of the adsorbed species with the material surface, and the peak areas correspond to the amount of adsorbed species. Fig.3d shows that the binding strength of HCl with various graphene materials increases in the following order: GO < N-G < B, N-G. The desorption temperatures of the highest peak were 196.8, 219.2, and 275.5 °C, respectively. In addition, GO has a negligible HCl adsorption ability, implying that almost no catalytic active sites are found on this catalyst. Compared with the original GO without doping, the improvement of the adsorption performance of N-G highly depends on the considerably stronger interaction between N and HCl, thus validating the capability of N for directly activating HCl. A considerable HCl absorption occurred on B, N-G because of additional N content and stronger adsorption of HCl in the presence of B atoms, which explains the excellent acetylene conversion observed. These results support our theoretical observation from DFT calculations of the HCl adsorption and outstanding activity of the B, N-G.

Fig. 5 evidently shows that the acetylene conversion of B, N-G decreased from 94.89% to 61.88% within 4 h, indicating its poor catalytic stability during acetylene hydrochlorination. The decrease of activity was due to the severe deactivation of catalyst. It was confirmed that the coke formation covered on the active sites was the main reason for deactivation according to the TGA results as showed in Fig. 6. TGA was used to evaluate the degree of carbon deposition on the surface of catalysts, which based on previous reported calculation method [10]. In generally, there have

two parts of mass loss within 100-500 °C; first, the burning of coke deposition on the catalyst surface; second, the oxidation of carbon carrier in the atmosphere and then escaping as CO₂. Therefore, the amount of carbon deposition should be equal to the difference of the mass loss between the fresh and used catalysts in the temperature range of 100-500 °C. The mass loss of the spent B, N-G is 5.0 wt.% higher than that of the fresh B, N-G catalyst within the 100 °C to 500 °C. This result indicates that coke deposition occurs on the B, N-G catalyst as the reaction proceeds. Therefore, coke deposition may be the reason for the deactivation of B, N-G in acetylene hydrochlorination. To reactivate the covered active sites, burning off the coke with hydrogen in 600 °C was studied. After the first regeneration, the activity curve implied initial acetylene conversion recover to 93% although the acetylene conversion decreased rapidly as the reaction went on 60 min, which demonstrated well recovery ability. The second regeneration was employed again to recover the activity of the deactivated B, N-G catalyst. However, the initial acetylene conversion partially recovers to 82%, which may be caused by the insufficient regeneration. Overall, burning off the deactivated B, N-G catalyst with hydrogen in 600 °C is an available technique in recovering activity.

4. Conclusions

In summary, B, N-G catalyst was prepared and applied in acetylene hydrochlorination. This catalyst exhibited high activity for acetylene conversion, reaching 94.87%, and is selective to vinyl chloride (above 98%) with GHSV (C₂H₂) of 36 h⁻¹ and at 150 °C. The enhanced catalytic activity of B, N-G catalyst may be

attributed to the improved HCl adsorption, which is proved by the DFT calculation and TPD experiment. Therefore, B, N-G is a promising catalyst for acetylene hydrochlorination because of its high catalytic efficiency and relatively low cost.

Acknowledgments

This work was supported by the National Basic Research Program of China (973Program, 2012CB720302), the Program for Changjiang Scholars and Innovative Research Teams in University (PCSIRT, IRT1161), and National Natural Science Funds of China(NSFC, 21366027).

References

- [1] Li, X.; Zhu, M.; Dai, B. *Appl. Catal. B-Environ.* **2013**, 142, 234-240.
- [2] Hutchings, G.J.; Haruta, M. *Appl. Catal. A- Gen.* **2005**, 291, 2-5.
- [3] Smith, D.; Walsh, P.; Slager, T. *J. Catal.* **1968**, 11, 113-130.
- [4] Mitchenko, S.A.; Krasnyakova, T.V.; Mitchenko, R.S.; Korduban, A.N. *J. Mol. Catal. A- Chem.* **2007**, 275, 101-108.
- [5] Nkosi, B.; Adams, M.D.; Coville, N.J.; Hutchings, G.J. *J. Catal.* **1991**, 128, 378-386.
- [6] Hutchings, G.J. *Catal. Today* **2002**, 72, 11-17.
- [7] Nkosi, B.; Coville, N.J.; Hutchings, G.J.; Adams, M.D.; Friedl, J.; Wagner, F.E. *J. Catal.* **1991**, 128, 366-377.
- [8] Conte, M.; Carley, A.F.; Heirene, C.; Willock, D.J.; Johnston, P.; Herzing, A.A.; Kiely, C.J.; Hutchings, G.J. *J. Catal.* **2007**, 250, 231-239.
- [9] Zhang, H.; Dai, B.; Wang, X.; Xu, L.; Zhu, M. *J. Ind. Eng. Chem.* **2012**, 18, 49-54.

- [10] Zhang, H.; Dai, B.; Wang, X.; Li, W.; Han, Y.; Gu, J.; Zhang, J. *Green Chem.* **2013**, 15, 829-836.
- [11] Huang, C.; Zhu, M.; Kang, L.; Li, X.; Dai, B. *Chem. Eng. J.* **2014**, 242, 69-75.
- [12] Li, X.; Wang, Y.; Kang, L.; Zhu, M.; B. Dai, *J. Catal.* **2014**, 311, 288-294.
- [13] Zhou, K.; Li, B.; Zhang, Q.; Huang, J.Q.; Tian, G.L.; Jia, J.C.; Zhao, M.Q.; Luo, G.H.; Su, D.S.; Wei, F. *ChemSusChem* **2014**, 7, 723-728.
- [14] Li, X.; Pan, X.; Yu, L.; Ren, P.; Wu, X.; Sun, L.; Jiao, F.; Bao, X. *Nat. Commun.* **2014**, 5, 3688-3694.
- [15] Wang, H.; Maiyalagan, T.; Wang, X. *ACS Catal.* **2012**, 2, 781-794.
- [16] Jiao, Y.; Zheng, Y.; Jaroniec, M.; Qiao, S.Z. *J. Am. Chem. Soc.* **2014**, 136, 4394-4403.
- [17] Deng, D.; Pan, X.; Yu, L.; Cui, Y.; Jiang, Y.; Qi, J.; Li, W.X.; Fu, Q.; Ma, X.; Xue, Q. *Chem. Mater.* **2011**, 23, 1188-1193.
- [18] Zhao, Y.; Yang, L.; Chen, S.; Wang, X.; Ma, Y.; Wu, Q.; Jiang, Y.; Qian, W.; Hu, Z. *J. Am. Chem. Soc.* **2013**, 135, 1201-1204.
- [19] Stankovich, S.; Dikin, D.A.; Dommett, G.H.; Kohlhaas, K.M.; Zimney, E.J.; Stach, E.A.; Piner, R.D.; Nguyen, S.T.; Ruoff, R.S. *Nature* **2006**, 442, 282-286.
- [20] Hummers Jr, W.S.; Offeman, R.E. *J. Am. Chem. Soc.* **1958**, 80, 1339-1339.
- [21] Su, Q.; Pang, S.; Alijani, V.; Li, C.; Feng, X.; Müllen, K. *Adv. Mater.* **2009**, 21, 3191-3195.
- [22] Park, S.; Ruoff, R.S. *Nat. Nanotechnol.* **2009**, 4, 217-224.
- [23] Li, D.; Müller, M.B.; Gilje, S.; Kaner, R.B.; Wallace, G.G. *Nat. Nanotechnol.*

2008, 3, 101-105.

[24] Becke, A.D. *J. Chem. Phys.* **1993**, 98, 5648-5652.

[25] Frisch, M.J.; Trucks, G. W.; Schlegel, H. B.; Scuseria, G. E.; Robb, M. A.; Cheeseman, J. R.; Scalmani, G.; Barone, V.; Mennucci, B.; Petersson, G. A., Gaussian 09, Revision C.01; Gaussian, Inc., Wallingford CT, (2010).

[26] Zheng, Y.; Jiao, Y.; Ge, L.; Jaroniec, M.; Qiao, S.Z. *Angew. Chem. Int. Edit.* **2013**, 125, 3192-3198.

[27] Niyogi, S.; Bekyarova, E.; Itkis, M.E.; Zhang, H.; Shepperd, K.; Hicks, J.; Sprinkle, M.; Berger, C.; Lau, C.N.; Deheer, W.A. *Nano Lett.* **2010**, 10, 4061-4066.

[28] Dikin, D.A.; Stankovich, S.; Zimney, E.J.; Piner, R.D.; Dommett, G.H.; Evmenenko, G.; Nguyen, S.T.; Ruoff, R.S. *Nature* **2007**, 448, 457-460.

[29] Ci, L.; Song, L.; Jin, C.; Jariwala, D.; Wu, D.; Li, Y.; Srivastava, A.; Wang, Z.; Storr, K.; Balicas, L. *Nat. Mater.* **2010**, 9, 430-435.

[30] Raymundo-Pinero, E.; Cazorla-Amorós, D.; Linares-Solano, A.; Find, J.; Wild, U. ; Schlögl, R. *Carbon* **2002**, 40, 597-608.

[31] Park, S.; Hu, Y.; Hwang, J.O.; Lee, E.S.; Casabianca, L.B.; Cai, W.; Potts, J.R.; Ha, H.W.; Chen, S.; Oh, J. *Nat. Commun.* **2012**, 3, 638-645.

Table 1 The calculated mass concentrations of different atoms in various graphenes^a.

Sample	C/%	O/%	N/%	B/%
GO	65.51	34.48	-	-
B-G	51.73	37.20	-	11.07
N-G	89.77	4.76	5.47	-
N-G (spent)	90.40	4.63	4.97	-
B, N-G	55.71	17.86	10.96	15.47
B, N-G (spent)	57.55	17.63	9.59	15.23

^aThe elemental composition and elemental content of catalysts were determined by XPS method.

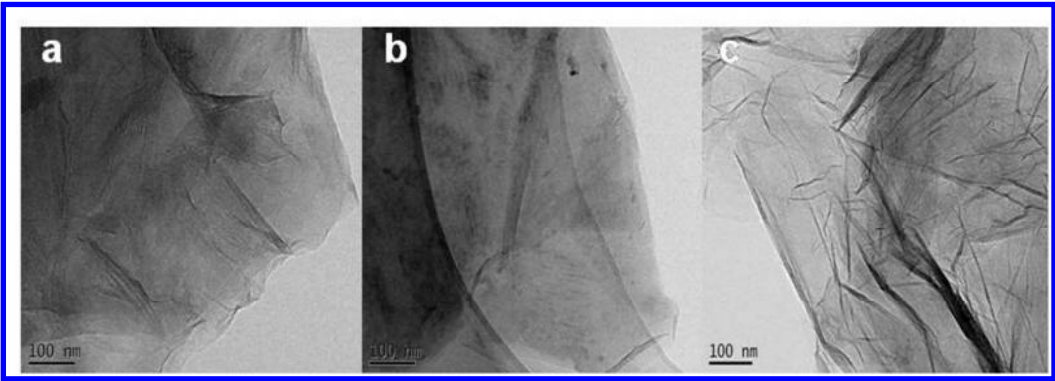
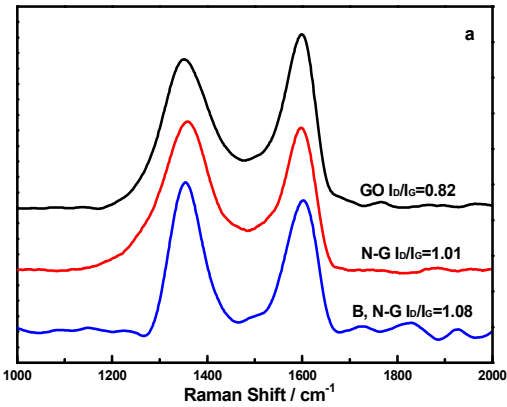


Fig.1 TEM images of: a) GO, b) N-G, c) B, N-G.



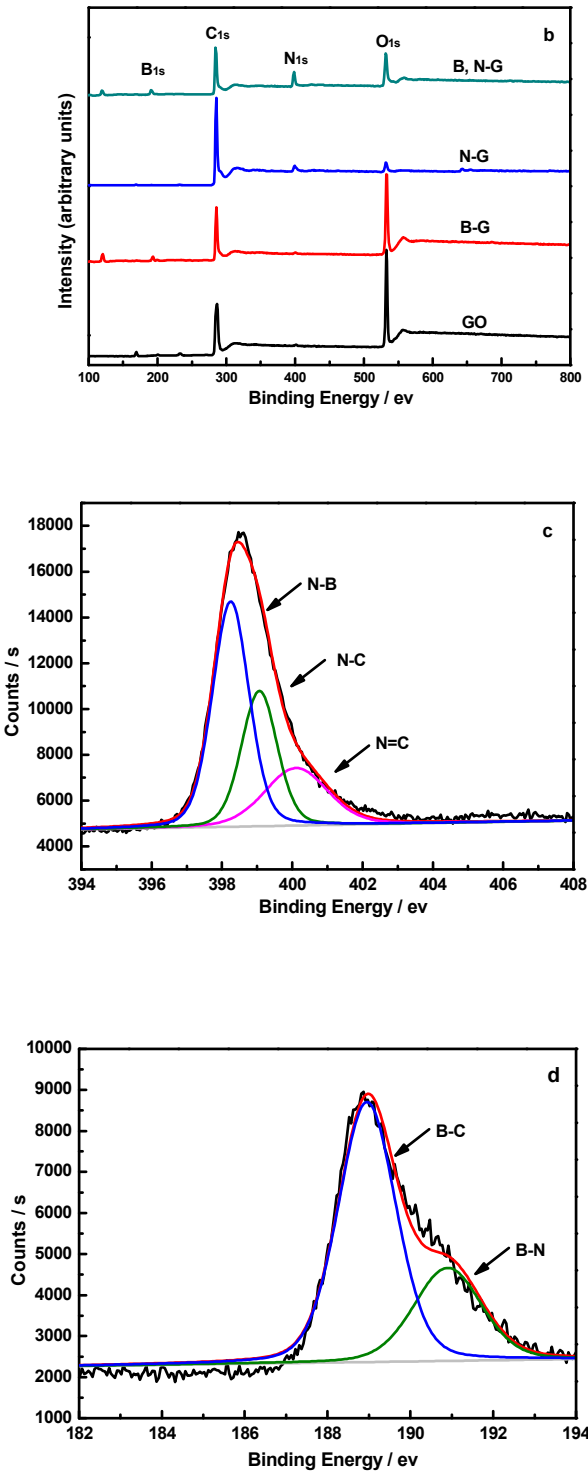
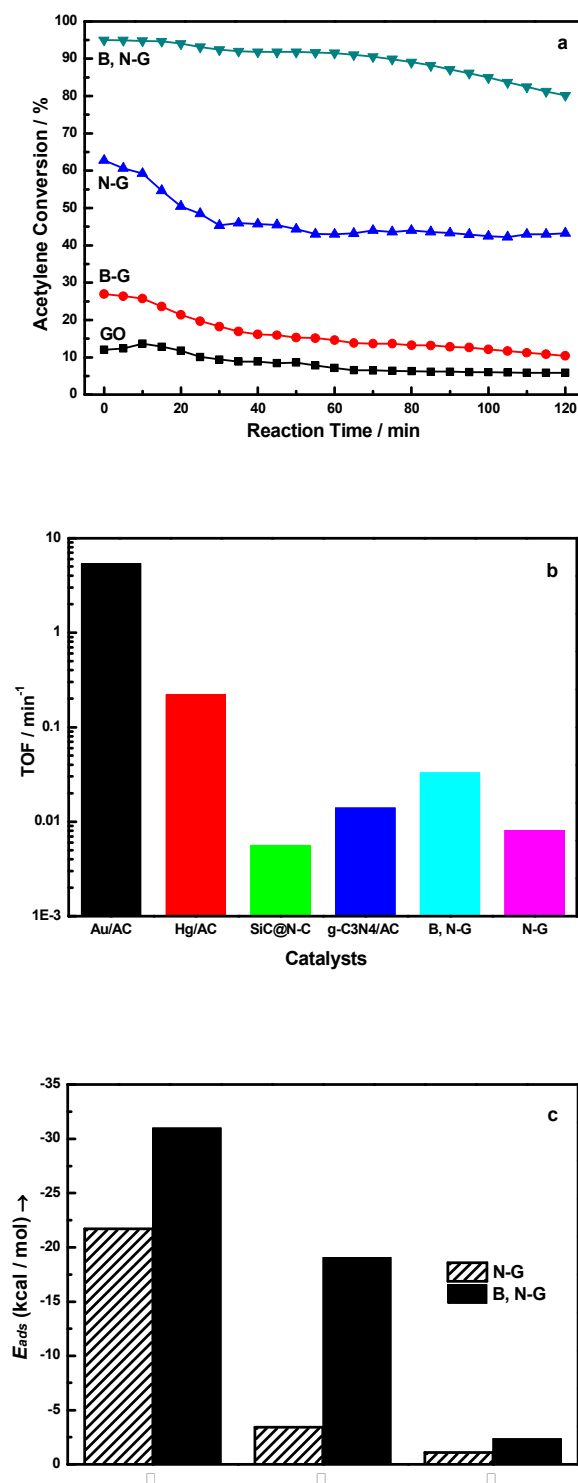


Fig.2 (a) Raman spectra for GO, N-G and B, N-G. (b) XPS survey spectra. (c) High-resolution N1s spectra of B, N-G. (d) High-resolution B1s spectra of B, N-G.



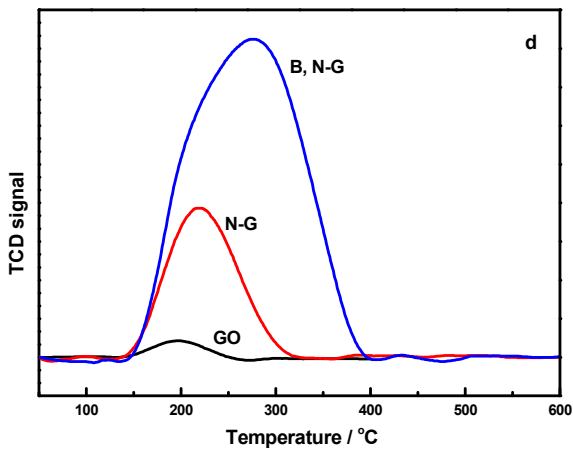


Fig.3 (a) Catalytic reactivity evaluation of: GO, B-G, N-G and B, N-G. Reactions were carried out at 150 °C, atmospheric pressure, a gas hourly space velocity (GHSV) of 36 h⁻¹, HCl/C₂H₂=1.15/1 (volume ratio). (b) The TOFs for different catalysts: Au/AC, Hg/AC, SiC@N-C, g-C₃N₄/AC, B, N-G, N-G. (c) *E*_{ads} of HCl on different types of active sites in N-G and B, N-G. I : The carbon atoms bonded with pyridinic N species. II : The carbon atoms bonded with pyrrolic N species. III: The carbon atoms bonded with graphitic N species. Please refer to Figure S3-S4 in the Supporting information for detailed molecular structures and the calculated HOMO states. (d) TPD profile of GO, N-G and B, N-G. The samples were pre-adsorbing by HCl gas for 2 h at a flow rate of 20 mL/min in the microreactor was heated to 150°C. Then it was taken out from the microreactor when the sample was cooling down to room temperature. Subsequently, Temperature-programmed desorption TPD was conducted using a Micromeritic ASAP 2720 instrument.

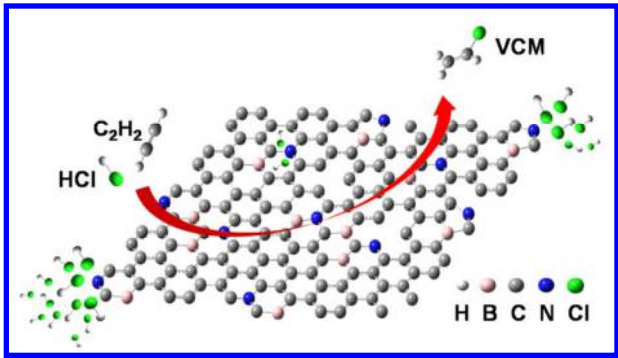


Fig. 4 Schematic illustration of acetylene hydrochlorination catalyzed by B, N-G catalysts.

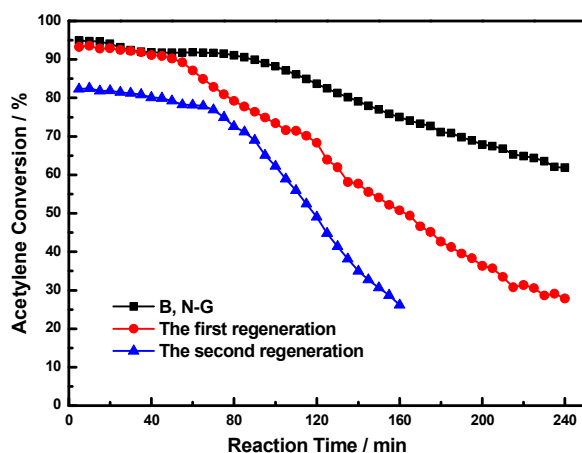


Fig.5 Conversion of acetylene during 4 h for B, N-G and regenerated B, N-G. The detailed regenerated condition: hydrogen atmosphere, 10 mL/min, 600 °C, 2 h.

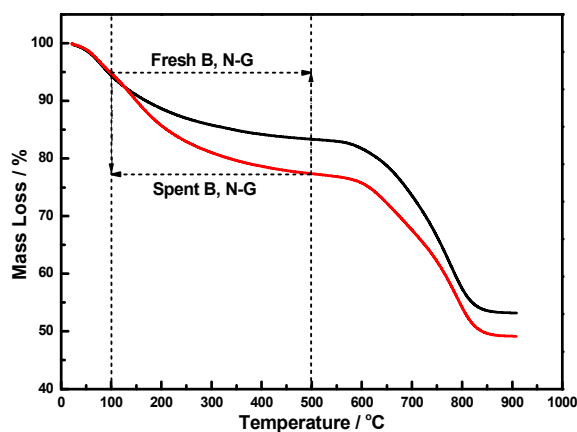


Fig.6 Thermogravimetric analysis curves recorded in air atmosphere of fresh B, N-G catalyst and spent B, N-G catalyst.

Table of contents (TOC)

